Nanotechnology **24** (2013) 075201 (8pp) doi:10.1088/0957-4484/24/7/075201

Size dependent competition between second harmonic generation and two-photon luminescence observed in gold nanoparticles

Hai-Dong Deng[1,2], Guang-Can Li[1], Qiao-Feng Dai[1], Min Ouyang[1], Sheng Lan[1], Vyacheslav A Trofimov[3] and Tatiana M Lysak[3]

[1] Laboratory of Nanophotonic Functional Materials and Devices, School of Information and Optoelectronic Science and Engineering, South China Normal University, Guangzhou 510006, People's Republic of China
[2] College of Science, South China Agricultural University, Guangzhou 510642, People's Republic of China
[3] Department of Computational Mathematics and Cybernetics, M V Lomonosov Moscow State University, Moscow 119992, Russia

E-mail: slan@scnu.edu.cn

Received 2 October 2012, in final form 5 December 2012
Published 28 January 2013
Online at stacks.iop.org/Nano/24/075201

Abstract
We investigate systematically the competition between the second harmonic generation (SHG) and two-photon-induced luminescence (TPL) that are simultaneously present in Au nanoparticles excited by using a femtosecond (fs) laser. For a large-sized (length ∼ 800 nm, diameter ∼ 200 nm) Au nanorod, the SHG appears to be much stronger than the TPL. However, the situation is completely reversed when the Au nanorod is fragmented into many Au nanoparticles by the fs laser. In sharp contrast, only the TPL is observed in small-sized (length ∼ 40 nm, diameter ∼ 10 nm) Au nanorods. When a number of the small-sized Au nanorods are optically trapped and fused into a large-sized Au cluster by focused fs laser light, the strong TPL is reduced while the weak SHG increases significantly. In both cases, the morphology change is characterized by scanning electron microscope. In addition, the modification of the scattering and absorption cross sections due to the morphology change is calculated by using the discrete dipole approximation method. It is revealed that SHG is dominant in the case when the scattering is much larger than the absorption. When the absorption becomes comparable to or larger than the scattering, the TPL increases dramatically and will eventually become dominant. Since the relative strengths of scattering and absorption depend strongly on the size of the Au nanoparticles, the competition between SHG and TPL is found to be size dependent.

(Some figures may appear in colour only in the online journal)

1. Introduction

Gold (Au) nanoparticles have been widely applied in various fields of science and technology because of their unique electronic, catalytic, optical, and plasmonic properties. These applications include surface enhanced Raman scattering [1–3], multi-dimensional optical data storage [4–6], biomedical imaging [7–9], biosensors [10–12], cancer therapy, etc [13, 14]. Among different Au nanoobjects, Au nanorods are of particular interest because of the strong

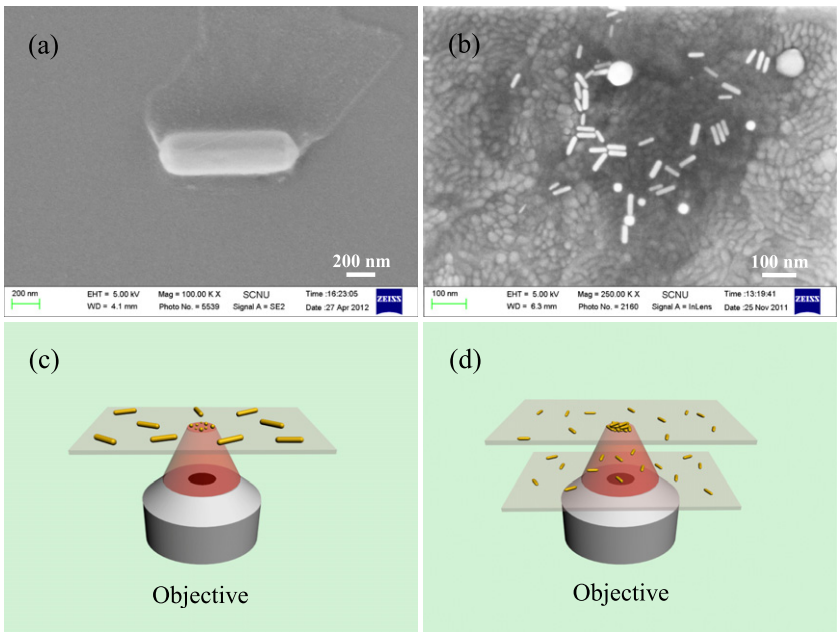

Figure 1. SEM images of a large-sized Au nanorod (a) and an ensemble of the small-sized Au nanorods (b) used in the experiments. Panels (c) and (d) show schematically the characterization of the nonlinear properties of the Au nanorods and the optical trapping and melting of the small-sized Au nanorods, respectively.

longitudinal surface plasmon resonance (LSPR) that can be tuned from the visible to the near infrared spectral region by varying the ratio of the length to the diameter.

Owing to the significant enhancement of the local electric field at the LSPR of Au nanorods, the nonlinear optical properties of Au nanorods are the subject of intensive and extensive research, especially the second harmonic generation (SHG) [15] and two-photon-induced luminescence (TPL) [16, 17] that are usually observed in Au nanorods excited by femtosecond (fs) laser pulses. Early in 1986, Boyd *et al* found that TPL, which depends quadratically on the excitation intensity, could be excited from rough metal surfaces and identified the origin of the TPL as the recombination of the electrons in the sp band with the holes in the d band [18]. Differently from TPL, SHG is not observed in metallic nanoparticles with centrosymmetry. Therefore, SHG depends strongly on defects, facets, and other small deviations from perfectly spherical shape. The SHG in nonlinear metamaterials such as split-ring resonators and other shapes of low symmetry has been investigated and it was found that defects and shape distortions might influence the SHG signal [19–26]. In addition, SHG scattering can occur from centrosymmetric particles by field retardation effects [27–29]. Nappa *et al* observed strong size dependent retardation effects in second harmonic scattering from gold or silver spheres and demonstrated that the SHG is due to the deviation of the particle shape from a perfect sphere [27, 28]. Polarization studies have shown that SHG can be enhanced via resonant excitation of the LSPR of Au nanorod arrays [30, 31].

In general, SHG and TPL are simultaneously present in Au nanoparticles excited by a fs laser. This implies that some of the energy of the fs laser is converted to SHG and some is transferred into TPL. Basically, SHG is a second-order nonlinear process and TPL is a third-order one. However, both of them scale quadratically with the intensity of the incident light, making the situation more complicated. Therefore, it is expected that there will exist a competition between these two processes. Thus, a key issue that needs to be clarified is what determines the energy distribution between these two processes. To the best of our knowledge, this issue remains unsolved. In this work, we investigate experimentally the competition between SHG and TPL in different Au nanoparticle systems, including Au nanorods with large and small sizes, Au nanoparticle arrays, and Au clusters with large sizes. By comparing the SHG and TPL observed in different Au nanoparticle systems with the scattering and absorption cross sections of these systems calculated by using the discrete dipole approximation (DDA) method [32], we reveal that the relative strengths of scattering and absorption, which are size dependent, determine the competition between SHG and TPL.

2. Sample preparation and experimental setup

Two types of Au nanorods with very different feature sizes (Nanopartz, Salt Lake City, UT) were used in the experiments. The average diameter and length of the large-sized Au nanorods were ∼200 and ∼800 nm while those of the small-sized ones were ∼10 and ∼40 nm. SEM images of a large-sized Au nanorod and an ensemble of small-sized Au nanorods are presented in figures 1(a) and (b), respectively. For the characterization of the nonlinear properties, uniformly distributed Au nanorods were obtained by dropping an aqueous solution of the Au nanorods onto a glass slide. The fs laser light from a Ti:sapphire oscillator (Mira 900S, Coherent) with a pulse duration of 130 fs and a repetition rate of 76 MHz was focused on the Au nanorods by using the objective

lens (100×, NA = 1.43) of an inverted microscope (Axio Observer A1, Zeiss), as schematically shown in figure 1(c). In all measurements, we carefully compared the SHG and TPL signals detected in a position with Au nanorods with that without Au nanorods (bare glass slide). Under the maximum excitation densities we used in the experiments, we did not observe any obvious SHG and TPL from the glass slide, indicating that the nonlinear response of the glass slide could be neglected. The vertical resolution of the microscope was 200 nm and the maximum nonlinear signals were found when the laser light was focused slightly above the glass slide where the Au nanorods were located. For optical trapping experiments, a 50 μm-thick sample cell filled with an aqueous solution of the small-sized Au nanorods with a concentration of ∼0.0036% was used, as illustrated in figure 1(d). In both cases, the emitted SHG and/or TPL signals were collected by using the same objective lens and directed into a spectrometer (SR-500i-B1, Andor) equipped with a charge-coupled device (CCD). In this case, the TPL observed for the small-sized Au nanorods suspended in water was quite similar to that observed for the small-sized Au nanorods placed on the glass slide, implying that the contribution of the glass slide to the nonlinear signals was negligible. The fragmentation of the large-sized Au nanorods and the trapping and melting of the small-sized Au nanorods could be easily monitored by using either the dark field mode of the microscope or the CCD attached on the microscope.

3. Results and discussion

3.1. Comparison of the nonlinear response between large-sized and small-sized Au nanorods

First, let us compare the nonlinear optical properties of the large-sized and small-sized Au nanorods under the excitation of a fs laser. The nonlinear response spectra in the visible to near infrared region for the two types of Au nanorods are compared in figure 2(a). It is observed that the spectrum for the large-sized nanorods is dominated by SHG while that for the small-sized ones is governed by TPL. The TPL emitted from the large-sized Au nanorods is quite weak as compared to the SHG. In sharp contrast, the SHG is almost invisible in the small-sized Au nanorods that emit very strong TPL. In figure 2(a), it is noticed that the TPL of the small-sized Au nanorods begins at ∼390 nm which is about 10 nm smaller than the wavelength corresponding to two photons of the fundamental (800 nm). Actually, a similar phenomenon was observed in previous literature concerning the TPL of Au nanorods but no explanation was given for it [7]. We think that more experiments are needed in order to clarify this issue, but they are beyond the scope of the present work. In order to understand the physical origin of the difference in nonlinear response, we calculated the extinction, absorption and scattering spectra for the two types of nanorods by using the DDA method [32], as shown in figures 2(b) and (c), where Q_{ext}, Q_{abs} and Q_{sca} are the extinction, absorption and scattering efficiencies, respectively [33]. The numerical simulations were performed for the large-sized Au nanorods surrounded by air and the small-sized nanorods surrounded by water. The effect of a substrate, which is thought to have little influence on the conclusions drawn in this paper, was not taken into account. If the surrounding medium is changed, for example from air to glass or polymer, the major effect is a shift of the surface plasmon resonance peak. In figures 2(b) and (c), it is noticed that the extinction for the large-sized nanorods is dominated by scattering while that for the small-sized ones is governed by absorption. Since TPL involves the generation of real carriers due to the absorption of fs laser light while SHG does not, it is easily understood that the difference in nonlinear response between these two types of nanorods is mainly caused by the relative strengths of scattering and absorption. This phenomenon suggests that SHG is dominant in large-sized nanoparticles whose scattering is much larger than their absorption while TPL is dominant in small-sized nanoparticles in which scattering is negligible as compared to absorption.

To gain a deep insight into the effect of particle size on the local electric field enhancement, we calculated the electric field distributions at an excitation wavelength of 800 nm for the large-sized and small-sized nanorods, and the results in the *xy* plane are compared in figures 2(d) and (e). For small-sized nanorods, a significant enhancement in electric field can be clearly observed due to the coincidence of the excitation wavelength with the LSPR of the nanorods (see the color scale bar). In sharp contrast, the enhancement in electric field appears to be much smaller for large-sized nanorods because of a broad scattering spectrum spanning from the visible to the near infrared region.

In order to verify the conclusion drawn above, we performed two experiments. In the first experiment, a large-sized nanorod was fragmented into a number of small-sized nanoparticles by irradiating fs laser light with a sufficiently large energy density and the change in nonlinear response was examined. In the second one, a number of small-sized nanorods were optically trapped and fused into a large-sized cluster by using focused fs laser light and the change in nonlinear response was monitored.

3.2. Fragmentation of a large-sized nanorod into a number of small-sized nanoparticles

As schematically shown in figure 1(c), the nonlinear response of a single large-sized nanorod can be characterized by focusing fs laser light on it and detecting the nonlinear signal. The evolution of the nonlinear spectrum with increasing excitation density is shown in figure 3(a). At low excitation densities, the nonlinear spectrum is completely dominated by SHG which increases quadratically with increasing excitation density. This behavior is consistent with the second-order nonlinear process nature of SHG. When the excitation density is raised to 1.2×10^4 W cm^{-2}, a significant increase of TPL from 155 to 1080, which is accompanied with a dramatic reduction of SHG from 2600 to 235, is observed. This phenomenon is clearly manifested in the evolution of the SHG and TPL intensities with increasing excitation density shown in figure 3(b). In the case when both SHG and TPL

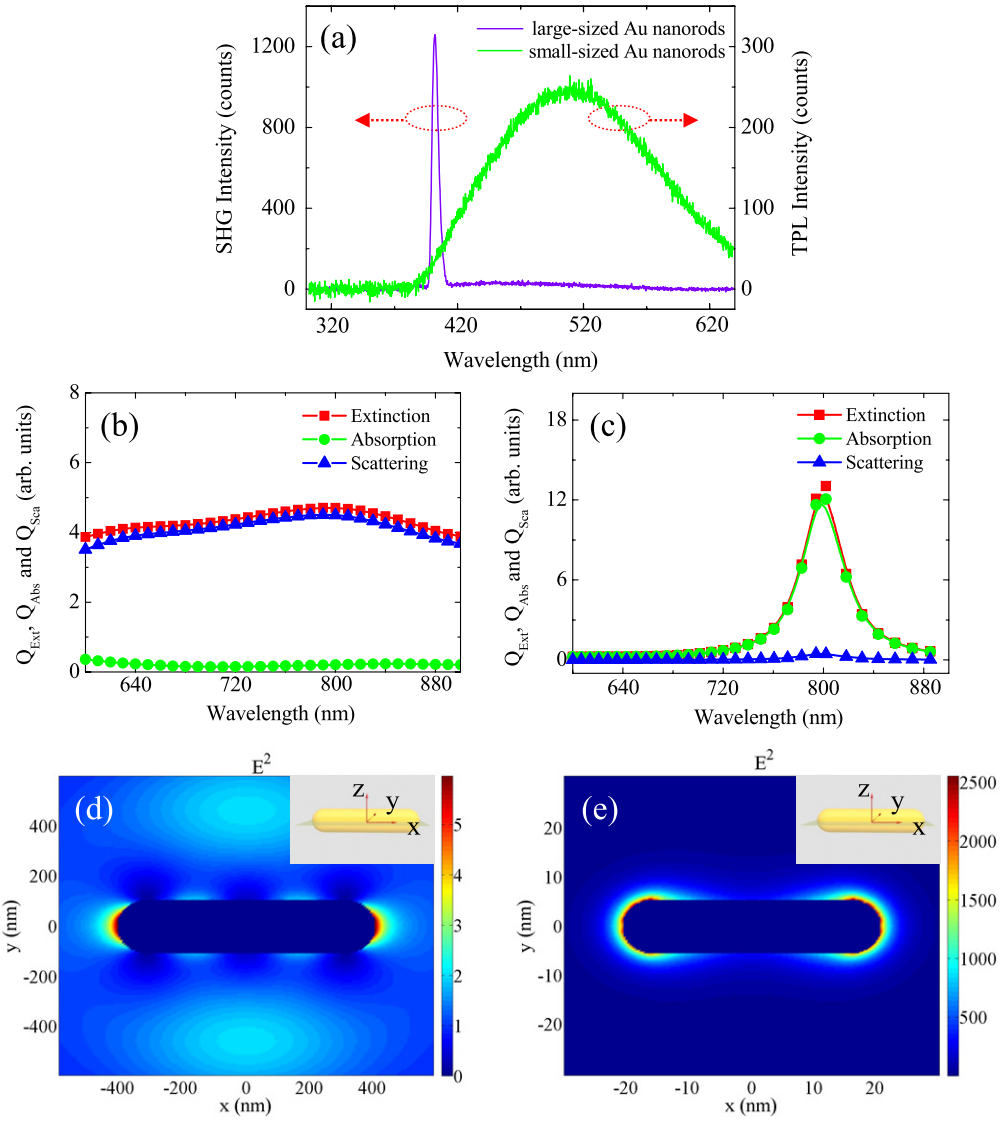

Figure 2. (a) Nonlinear response spectra of the two types of Au nanorods. The calculated extinction, absorption and scattering spectra for the large-sized and small-sized Au nanorods are shown in (b) and (c) while the corresponding electric field intensity distributions in the *xy* plane around the nanorods are shown in (d) and (e), respectively. The insets in (d) and (e) show the coordinates indicating the alignment of the nanorods. The light is polarized in the *x* direction and incident on the nanorods in the *z* direction.

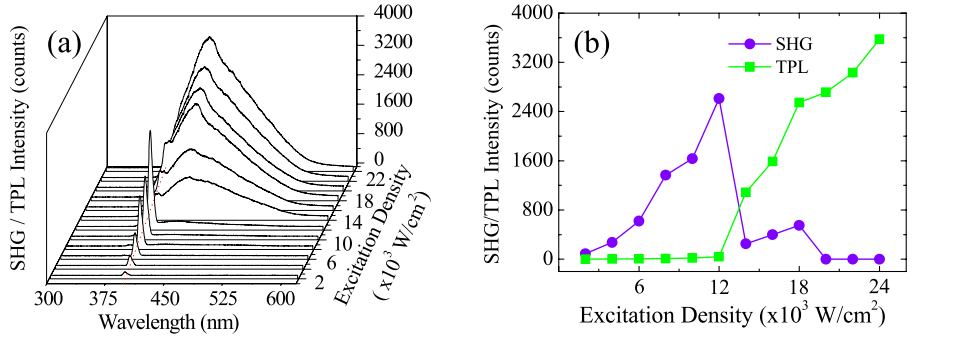

Figure 3. Evolution of the nonlinear response spectrum (a) and the SHG and TPL intensities (b) of the large-sized Au nanorod with increasing excitation density of the fs laser.

are present, we extracted the SHG signal by either fitting the spectrum with multiple Gaussian peaks or assuming the TPL spectrum was continuous. In both cases, the extracted SHG signal was similar and we chose the former one. At high excitation densities, the nonlinear spectrum is completely dominated by the TPL and the SHG becomes almost invisible.

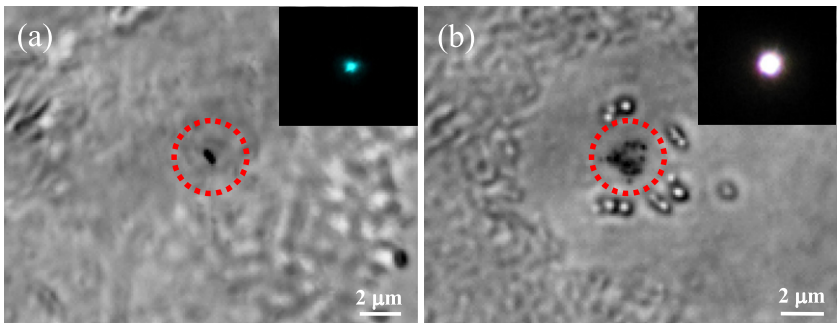

Figure 4. CCD images showing the fragmentation of a large-sized Au nanorod into a number of randomly distributed Au nanoparticles.

The fragmentation experiment was performed by using a fs laser with a high repetition rate (76 MHz). It was found that the laser excitation density played a dominant role. In experiments, we increased the excitation density with an interval of $\sim 2 \times 10^3$ W cm^{-2} and monitored the fragmentation process of the Au nanorods. It was found that fragmentation did not occur for excitation densities below a critical level ($\sim 1.2 \times 10^4$ W cm^{-2}) no matter how many pulses were irradiated. The fragmentation experiments were carried out for many nanorods. The threshold excitation density for fragmentation and the morphology of the nanoparticles after fragmentation were found to be different for different nanorods, as shown in the following. For excitation densities larger than the critical level, fragmentation of nanorods was observed immediately once the fs laser pulses were irradiated on the nanorods. This was reflected in a change of the nonlinear response as well as the color of the emitting light. Since the repetition rate of the fs laser was very high (76 MHz), it was difficult to estimate the number of pulses that caused the fragmentation of the nanorods. Such a study needs the use of a fs amplifier with a low repetition rate and high peak power.

In order to find the physical origin responsible for the significant change in nonlinear response, we examined the morphology changes of the nanorods before and after the irradiation of fs laser light with high excitation densities by using the CCD connected to the microscope, as shown in figure 4. It can be seen that the large-sized nanorod was indeed fragmented into a number of randomly distributed nanoparticles that were dispersed in an area much larger than the original size of the nanorod. This indicates that the explosion of the nanorod was caused by a multiphoton ionization process induced by the absorption of the fs laser light [34]. When comparing the images shown in figures 4(a) and (b), some bright features are observed in figure 4(b) after the fragmentation of the nanorod. In the preparation of Au nanorods, a certain kind of surfactant (e.g., cetyltrimethylammonium bromide) is usually used in order to prevent them from agglomeration. Some surface surfactant will be left on the surfaces of the Au nanorods and the glass slide after the evaporation of water, as shown in figure 1(a). It is impossible to completely remove the surface surfactant. Therefore, we think that the bright features appearing in figure 4(b) are small islands of surface surfactant generated during the fragmentation of the nanorod because the large amount of heat released in the process leads to a significant rise in temperature. During the experiments, however, we carefully compared the response of the region with nanoparticles with that without nanoparticles and confirmed that the nonlinear signals really originated from the nanoparticles and the contribution from the surfactant and substrate was negligible. The diameter of the laser spot was only 1–2 μm and the nonlinear response as well as the bright TPL disappeared when we moved the laser spot out of the region with nanoparticles. In the insets of figure 4, we also present photos of the emitted light taken from the eyepiece of the microscope just before and after the fragmentation of the nanorod. It was found that the large-sized nanorod emitted blue light with a small spot size while the randomly distributed nanoparticles emitted white light with a much larger spot size. The color of the emitted light was consistent with the nonlinear spectrum shown in figure 3.

Based on SEM observation, we were able to investigate in detail the fragmentation of large-sized Au nanorods. In figure 5, we show two different fragmentation processes of large-sized Au nanorods: partial fragmentation (figure 5(a)) and complete fragmentation (figure 5(b)). In figure 5(a), only part of the nanorod was fragmented into nanoparticles and the fragmentation was observed at an excitation density of $\sim 1.8 \times 10^4$ W cm^{-2}. In this case, it is thought that the laser beam was not focused exactly at the center of the nanorod. As a result, the fragmentation occurred only in the lower part of the nanorod and the upper part remained nearly unaffected. In contrast, it can be seen in figure 5(b) that a large-sized nanorod has been completely transformed into nanospheres with different sizes ranging from 10 to 80 nm. In this case, the excitation density we used was $\sim 1.2 \times 10^4$ W cm^{-2} and the laser spot was accurately positioned at the center of the nanorod.

3.3. Optical trapping and fusion of small-sized Au nanorods into a large-sized Au cluster

Now let us move on to the second experiment in which a large number of the small-sized Au nanorods suspended in water were optically trapped and fused into a large-sized Au cluster. In this case, focused fs laser light with an excitation density of $\sim 1.2 \times 10^4$ W cm^{-2} was employed not only to trap nanorods but also to excite the nonlinear signals of the trapped nanorods. In figure 6, we present the evolution of

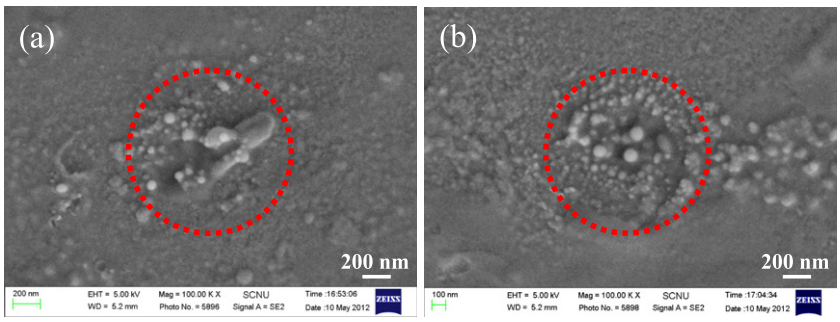

Figure 5. SEM images showing a partially fragmented (a) and a completely fragmented (b) large-sized Au nanorod.

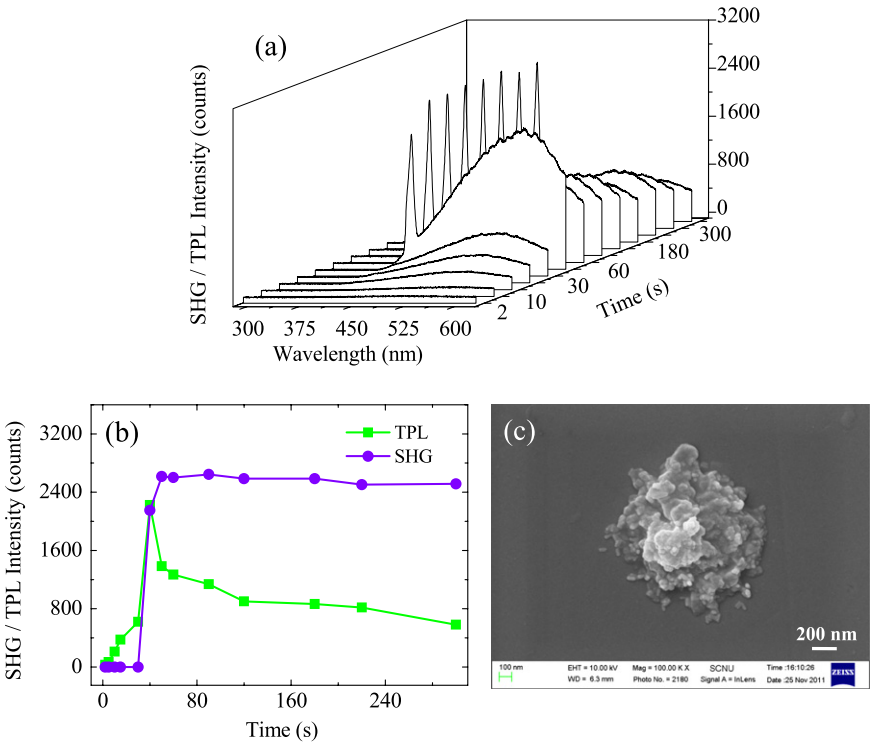

Figure 6. Evolution of the nonlinear response spectrum (a) and the TPL and SHG signals (b) after switching on the fs laser light. (c) SEM image of a large-sized Au cluster formed by optical trapping and fusion of the small-sized Au nanorods.

the nonlinear response spectrum of the trapped nanorods with time after switching on the fs laser light. It can be seen that the TPL intensity increases rapidly ∼10 s after turning on the laser light. This implies that many nanorods have been trapped at the focus by the gradient force of the focused laser light. It is noticed, however, that an extremely strong SHG signal with a peak intensity of ∼2200 appears suddenly at ∼30 s. After that, the SHG intensity remains nearly unchanged while the TPL intensity decreases gradually. We plot the evolution of the TPL and SHG intensities with time in figure 6(b), where a sharp increase in the SHG intensity is identified at ∼30 s. In order to find the physical origin for the sharp increase of SHG, the nanostructure formed on the top wall of the sample cell at the focus position was examined by SEM, and a large-sized cluster with a mountain shape was observed, as shown in figure 6(c). The base diameter of the cluster was estimated to be ∼1100 nm. It is suggested that the strong SHG originated from the large-sized cluster which was formed by the melting of the small-sized nanorods. In contrast to the phenomenon shown in figure 3(b), where a sharp increase in TPL is accompanied by a dramatic reduction in SHG, only a gradual reduction in TPL is observed in this case because more and more nanorods are being trapped into the focal volume, compensating partly the quenching of the TPL from the melted nanorods. In figure 6(c), one can see some unmelted Au nanorods distributed randomly on the surface of the cluster. They are responsible for the stable TPL even 5 min after switching on the laser light.

The small-sized nanorods were optically trapped in the focus of the laser light and fused into a large cluster. This process occurred in water. Since the small-sized nanorods could efficiently absorb fs laser light, they were melted into spheres and then fused into a large cluster. Fragmentation appeared for large nanorods which were directly irradiated by a fs laser in air. For large-sized nanorods in which the absorption is not efficient, the multiphoton ionization process

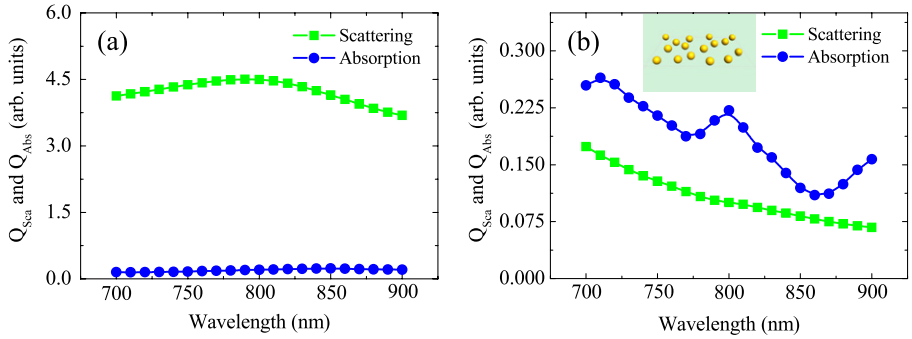

Figure 7. The relative strengths of scattering and absorption for the large-sized Au nanorod (a) and the randomly distributed small-sized Au nanoparticles (b). The inset in (b) shows the sixteen randomly distributed nanospheres (with a diameter of 64 nm and a mean separation of 100 nm) used to simulate the fragmentation of the large-sized nanorod into a number of randomly distributed nanoparticles, as shown in figure 4.

is dominant, leading to explosion of the large-sized nanorod. The physical mechanism for this process has been discussed previously [34].

3.4. Discussion

Basically, the local field factor $L(\omega)$ is related to the light extinction as follows [16, 18]:

$$I_{\text{ext}}(\omega) = I_{\text{abs}}(\omega) + I_{\text{sca}}(\omega) \approx N(\alpha(\omega) + \beta(\omega))L^2(\omega)I_{\text{in}}. \quad (1)$$

Here, I_{ext}, I_{abs}, I_{sca}, and I_{in} are the intensities of extinction, absorption, scattering, and incident light respectively; $\alpha(\omega)$ and $\beta(\omega)$ are the intrinsic constants of absorption and scattering; N is the number of Au nanoparticles in the laser light path. From equation (1), it can be seen that the absorption and scattering, which are determined by the intrinsic coefficients of absorption and scattering respectively, are the major two processes that deplete the incident light intensity. On the other hand, optical absorption and scattering of Au nanoparticles have dominant effects on the nonlinear processes of Au nanoparticles, such as SHG and TPL.

In figures 2(d) and (e), we compared the local electric field distributions of the two types of Au nanorods and found that the electric field enhancement for the small-sized nanorods appears to be much larger than that for the large-sized ones because of the coincidence of the excitation wavelength with the LSPR of the small-sized nanorods. The large enhancement in electric field together with the large absorption leads to the strong TPL observed in the small-sized nanorods.

Based on the experimental results described above, it is suggested that there exists a competition between SHG and TPL in a nanoparticle system excited by fs laser light. Since TPL involves the generation of real carriers while SHG does not, it is thought that TPL and SHG are governed by the absorption and scattering of the nanoparticle system, respectively. Thus, the competition between them is determined by the relative strengths of absorption and scattering in the nanoparticle system. In figure 7, we show the scattering and absorption spectra calculated by using the DDA method for a large-sized Au nanorod as well as for sixteen randomly distributed Au nanospheres (with a diameter of 64 nm and a mean separation of 100 nm and surrounded by air) used to simulate the fragmentation of the large-sized nanorod into a number of randomly distributed nanoparticles, as shown in figure 4. For the large-sized Au nanorod, it can be seen that the scattering is much larger than the absorption. Therefore, the nonlinear response spectrum is dominated by SHG. When the large-sized nanorod is fragmented into a number of randomly distributed nanospheres, the scattering is reduced significantly while the absorption is increased slightly. Consequently, the absorption becomes comparable to the scattering, as shown in figure 7(b). This change in relative strength is responsible for the sharp increase in TPL observed in the experiment.

Based on the experimental observations and numerical simulations presented above, it is suggested that the size of particles rather than their shape plays a dominant role in the competition between SHG and TPL. For particles with small sizes, it is difficult to observe SHG. However, for particles whose shape is of low symmetry, SHG can be observed if their size is large enough. Of course, for particles with sufficiently large sizes, low symmetry in shape or distortion may have influence on SHG.

4. Summary

We have investigated the nonlinear responses of different Au nanoparticle systems, including large-sized nanorods, small-sized nanorods, randomly distributed nanospheres, and large-sized clusters under the excitation of fs laser light. The extinction, scattering, and absorption spectra of these systems have been calculated by using the DDA method. A competition between SHG and TPL is experimentally observed. It is found that there exists a strong correlation between the scattering of the nanoparticle system and the SHG. A similar correlation is also found between the absorption of the nanoparticle system and the TPL. Therefore, it is suggested that SHG is determined by the scattering while TPL is governed by the absorption of the nanoparticle system. The competition is determined by the relative strengths of scattering and absorption. This conclusion is

verified experimentally by two experiments in which the relative strengths of scattering and absorption are intentionally modified by changing the size of the nanoparticle system. The results presented in this work are helpful for understanding the nonlinear optical properties of various metallic nanoparticle systems and exploring their possible applications in the fabrication of nanometer-sized devices.

Acknowledgments

The authors acknowledge the financial support from the National Natural Science Foundation of China (Grant Nos 10974060, 51171066 and 11111120068), the Ministry of Education (Grant No. 20114407110002) and the program for high-level professionals in the universities of Guangdong province, China. H D Deng would like to acknowledge the financial support from the Natural Science Foundation of Guangdong province (Grant No. S2012040007719).

References

[1] Nie S and Emory S R 1997 *Science* **275** 1102–6
[2] Huang X, El-Sayed I H, Qian W and El-Sayed M A 2007 *Nano Lett.* **7** 1591–7
[3] Qian X, Peng X H, Ansari D O, Yin-Goen Q, Chen G Z, Shin D M, Yang L, Young A N, Wang M D and Nie S 2008 *Nature Biotechnol.* **26** 83–90
[4] Zijlstra P, Chon J W M and Gu M 2009 *Nature* **459** 410–3
[5] Chon J W M, Bullen C, Zijlstra P and Gu M 2007 *Adv. Funct. Mater.* **17** 875–80
[6] Li X, Lan T H, Tien C H and Gu M 2012 *Nature Commun.* **3** 998
[7] Wang H, Huff T B, Zweifel D A, He W, Low P S, Wei A and Cheng J X 2005 *Proc. Natl Acad. Sci. USA* **102** 15752–6
[8] Durr N J, Larson T, Smith D K, Korgel B A, Sokolov K and Ben-Yakar A 2007 *Nano Lett.* **7** 941–5
[9] Huang X, El-Sayed I H, Qian W and El-Sayed M A 2006 *J. Am. Chem. Soc.* **128** 2115–20
[10] EL-Sayed I H, Huang X and El-Sayed M A 2005 *Nano Lett.* **5** 829–34
[11] Yu C and Irudayaraj J 2007 *Anal. Chem.* **79** 572–9
[12] Mayer K M, Lee S, Liao H, Rostro B C, Fuentes A, Scully P T, Nehl C L and Hafner J H 2008 *ACS Nano* **2** 687–92
[13] Huang Y F, Sefah K, Bamrungsap S, Chang H T and Tan W 2008 *Langmuir* **24** 11860–5
[14] Eghtedari M, Liopo A V, Copland J A, Oraevsky A A and Motamedi M 2009 *Nano Lett.* **9** 287–91
[15] Hubert C, Billot L, Adam P M, Bachelot R, Royer P, Grand J, Gindre D, Dorkenoo K D and Fort A 2007 *Appl. Phys. Lett.* **90** 181105
[16] Wang D S, Hsu F Y and Lin C W 2009 *Opt. Express* **17** 11350–9
[17] Imura K, Nagahara T and Okamoto H 2005 *J. Phys. Chem.* B **109** 13214–20
[18] Boyd G T, Yu Z H and Shen Y R 1986 *Phys. Rev.* B **33** 7923–36
[19] Klein M W, Enkrich C, Wegener M and Linden S 2006 *Science* **313** 502–4
[20] Feth N *et al* 2008 *Opt. Lett.* **33** 1975–7
[21] Kujala S, Canfield B K, Kauranen M, Svirko Y and Turunen J 2007 *Phys. Rev. Lett.* **98** 167403
[22] Czaplicki R, Zdanowicz M, Koskinen K, Laukkanen J, Kuittinen M and Kauranen M 2011 *Opt. Express* **19** 26866–71
[23] Canfield B K, Husu H, Laukkanen J, Bai B, Kuittinen M, Turunen J and Kauranen M 2007 *Nano Lett.* **7** 1251–5
[24] Canfield B K, Kujala S, Jefimovs K, Turunen J and Kauranen M 2004 *Opt. Express* **12** 5418–23
[25] Lesuffleur A, Swaroop Kumar L K and Gordon R 2006 *Appl. Phys. Lett.* **88** 261104
[26] Xu T, Jiao X, Zhang G P and Blair S 2007 *Opt. Express* **15** 13894–906
[27] Nappa J, Revillod G, Russier-Antoine I, Benichou E, Jonin C and Brevet P F 2005 *Phys. Rev.* B **71** 165407
[28] Nappa J, Russier-Antoine I, Benichou E, Jonin C and Brevet P F 2006 *J. Chem. Phys.* **125** 184712
[29] Butet J, Bachelier G, Russier-Antoine I, Jonin C, Benichou E and Brevet P F 2010 *Phys. Rev. Lett.* **105** 077401
[30] McMahon M D, Lopez R, Haglund R F Jr, Ray E A and Bunton P H 2006 *Phys. Rev.* B **73** 041401
[31] McMahon M D, Ferrara D, Bowie C T, Lopez R and Haglund R F Jr 2007 *Appl. Phys.* B **87** 259–65
[32] Draine B T and Flatau P J 2012 *User Guide for the Discrete Dipole Approximation Code DDSCAT 7.2* arXiv:1202.3424
[33] Lee K S and El-Sayed M A 2005 *J. Phys. Chem.* B **109** 20331–8
[34] Link S, Burda C, Mohamed M B, Nikoobakht B and El-Sayed M A 1999 *J. Phys. Chem.* A **103** 1165–70